The Maximum principle for Beltrami color flow

Lorina Dascal and Nir Sochen

Department of Applied Mathematics
University of Tel-Aviv, Ramat-Aviv, Tel-Aviv 69978, Israel
{lorina,sochen}@post.tau.ac.il

Abstract. We study, in this work, the maximum principle for the Beltrami color flow and the stability of the flow's numerical approximation by finite difference schemes. We discuss, in the continuous case, the theoretical properties of this system and prove the maximum principle in the strong and the weak formulations. In the discrete case, all the second order explicit schemes, that are currently used, violate, in general, the maximum principle. For these schemes we give a theoretical stability proof, accompanied by several numerical examples.

Keywords: Maximum Principle, Beltrami Framework, Parabolic PDE's, Finite difference schemes.

1 Introduction

The scale-space approach in low-level vision originated from several ideas: One point of view emphasized the multi-scale nature of images. Important features are to be found in all scale levels and one should use all scales in order to gain an understanding of the captured scene. The second, and somewhat related point of view, looked for a procedure of gradual simplification of the image. In each step the image should be a simplified version of the preceding step. New features, in a given step, that cannot be explained as a simplification of the previous step should not be present. This "causality" principle, introduced by Koenderink [11], leads directly to the maximum principle in the one-dimensional case.

Many generalizations of the scale-space linear flow exist. They are based on anisotropic and/or inhomogeneous diffusion flows. In order to serve as a basis for a multi scale analysis they should be "causal" flows. It is well known that the Perona-Malik continuous flow, for example, does not satisfy the maximum principle and cannot serve as a basis for a scale-space analysis. However, the closely related Partial Differential Equation (PDE) introduced by Catté, et al [2] has this property as does the discrete Perona-Malik flow [18].

There are several possible definitions of causality in higher dimensions. We restrict ourselves in this article to the study of the *maximum principle* feature for the color flow. We assume hereafter that the maximum principle is a necessary condition for causality. We treat in this paper the Beltrami flow for color images and show that it satisfies the maximum (minimum) principle in both the strong and the weak formulations.

We follow the duality approach of Florack [6] and treat an image as a tempered distribution. This approach follows our intuition that by taking two pictures of the scene with two different devices we have two representations of "the same thing" and not two completely different objects. The duality approach describes the sensor space as a functional space. The data that we usually process, which result from the interaction of the physical/optical data and the sensor, are modelled as an inner product of the sensor function and the "true image". Under this approach, the set of images is equivalent to the set of linear functionals on the sensor functional space (i.e. distributions). It is natural from this point of view to study the flow equations on the image space directly. In order to do that we have to define the equations in the weak sense. Another reason to study weak solutions is noise. Since noise is a non-continuous and non-differentiable function in all its points, the corrupted initial image which is a sum of the "true image" and the noise, is non-continuous and non-differentiable as well. One needs, then, to resort to the weak formulation in order to be able to *define* the PDE based denoising algorithm.

The strong formulation is presented here for two reasons. The first and obvious reason is that "it is there". Since we can prove it, then it fits naturally to the rest of this study. The second reason is more technical. It is used as an approximation tool in the proof of the maximum principle for weak solutions. We will prove below that if a weak solution exists then it must satisfy the maximum (minimum) principle.

In the last part of this paper we study the maximum principle for the various discrete schemes by which the differential equation is approximated. We show the fact that the various derivatives are approximated to a given order is not enough to guarantee the maximum principle. Many common numerical schemes are proved *to violate* the maximum principle. We present a proof, though, of their stability along with examples that clearly demonstrate their failure to obey the maximum principle.

The paper is organized as follows: In section 2 we review the Beltrami Framework. In section 3 we deal with the continuous formulation of the maximum principle. We present the maximum principle theorem for the strong solution of the parabolic quasilinear system that characterizes the Beltrami color flow. In section 4 we introduce the weak (distributional) solution for this system and present the maximum principle in a weak formulation. In section 5 we discuss the properties of the second-order central differences scheme, which in general violates the maximum principle. For this scheme we give a theoretical stability proof. In section 6 we present numerical results. We summarize and conclude in Section 7.

2 The Beltrami Framework

Let us briefly review the Beltrami framework for non-linear diffusion in computer vision [13, 14, 7].

We represent an image and other local features as embedding maps of a Riemannian manifold in a higher dimensional space. The simplest example is a gray-level image which is represented as a 2D surface embedded in $\mathbb{R}^3$. We denote the map by $X : \Sigma \to \mathbb{R}^3$. Where Σ is a two-dimensional surface, and we denote the local coordinates on it by (σ^1, σ^2). The map U is given in general by $(U^1(\sigma^1, \sigma^2), U^2(\sigma^1, \sigma^2), U^3(\sigma^1, \sigma^2))$. In our example we represent it as follows $(U^1 = \sigma^1, U^2 = \sigma^2, U^3 = I(\sigma^1, \sigma^2))$. We choose on this surface a Riemannian structure, namely, a metric. The metric is a positive definite and a symmetric 2-tensor that may be defined through the local distance measurements:

$$ds^2 = g_{11}(d\sigma^1)^2 + 2g_{12}d\sigma^1 d\sigma^2 + g_{22}(d\sigma^2)^2.$$

The canonical choice of coordinates in image processing is the cartesian. For such choice, that we follow in the rest of the paper we identify $\sigma^1 = x^1$ and $\sigma^2 = x^2$. We use below the Einstein summation convention in which the above equation reads $ds^2 = g_{ij}dx^i dx^j$ where repeated indices are summed over. We denote the elements of the inverse of the metric by superscripts $g^{ij} = (g^{-1})_{ij}$.

Once the image is defined as an embedding mapping of Riemannian manifolds it is natural to look for a measure on this space of embedding maps.

2.1 Polyakov Action: A measure on the space of embedding maps

Denote by (Σ, g) the image manifold and its metric and by (M, h) the space-feature manifold and its metric, then the functional $S[U]$ attaches a real number to a map $U : \Sigma \to M$:

$$S[U^a, g_{ij}, h_{ab}] = \int dV \langle \overrightarrow{\nabla} U^a, \overrightarrow{\nabla} U^b \rangle_g h_{ab}$$

where dV is a volume element and $\langle \nabla R, \nabla B \rangle_g = g^{ij}\partial_{x_i} R \partial_{x_j} B$. This functional, for $m = 2$ and $h_{ab} = \delta_{ab}$, was first proposed by Polyakov [12] in the context of high energy physics, and the theory known as *string theory*.

Let us formulate the Polyakov action in matrix form: (Σ, G) is the image manifold and its metric as before. Similarly, (M, H) is the spatial-feature manifold and its metric. Define

$$A^{ab} = (\overrightarrow{\nabla} U^a)^t G^{-1} \overrightarrow{\nabla} U^b$$

The map $U : \Sigma \to M$ has a weight

$$S[U, G, H] = \int d^m\sigma \sqrt{g} \mathrm{Tr}(AH),$$

where m is the dimension of Σ and $g = \det(G)$.

Using standard methods in the calculus of variations the Euler-Lagrange equations with respect to the embedding (assuming Euclidean embedding space) are (see [13] for explicit derivation):

$$-\frac{1}{2\sqrt{g}} h^{ab} \frac{\delta S}{\delta U^b} = \frac{1}{\sqrt{g}} \partial_{x_i}(\sqrt{g} g^{ij} \partial_{x_j} U^a).$$

Or in matricial form

$$-\frac{1}{2\sqrt{g}}h^{ab}\frac{\delta S}{\delta U^b} = \underbrace{\frac{1}{\sqrt{g}}\mathrm{div}\left(\sqrt{g}G^{-1}\nabla U^a\right)}_{\Delta_g U^a}. \tag{1}$$

The extension for non-Euclidean embedding space is treated in [14, 15, 8].

The elements of the induced metric for color images are:

$$g_{ij} = \delta_{ij} + \beta^2 \sum_{a=1}^{3} U^a_{x_i} U^a_{x_j}, \tag{2}$$

where $\beta > 0$ is the ratio between the spatial and color distances. Note that this metric is different from the Di Zenzo matrix [20](which is not a metric since it is not positive definite). A generalization of DiZenzo's gradient for color images has been investigated in [19] by constructing an anisotropic vector-valued diffusion model with a common tensor-valued structure descriptor.

The value of parameter β present in the elements of the metric g_{ij} is very important and determines the nature of the flow. In the limit $\beta \to 0$, for example, the flow degenerates to the decoupled channel by channel linear diffusion flow. In the other limit $\beta \to \infty$ we get a new non-linear flow. The gray-value analogue of this limit is the Total Variation flow of [9] (see details in [14]). Our proof of the extremum property is independent of the value of β though.

Since (g_{ij}) is positive definite, $g \equiv \det(g_{ij}) > 0$ for all σ^i. This factor is the simplest one that does not change the minimization solution while giving a reparameterization invariant expression. The operator that is acting on U^a is the natural generalization of the Laplacian from flat spaces to manifolds, is called the Laplace-Beltrami operator and is denoted by Δ_g.

The non-linear diffusion or scale-space equation emerges as a gradient descent minimization:

$$U^a_t = \frac{\partial}{\partial t}U^a = -\frac{1}{2\sqrt{g}}h^{ab}\frac{\delta S}{\delta U^b} = \Delta_g U^a. \tag{3}$$

The mathematical properties of this system, together with the initial value, given by the original noisy image and with Neumann boundary condition, are studied in the rest of the paper with an emphasis on the maximum principle.

3 Extremum Principle for Functional Solutions

We establish, in this subsection, the maximum principle for the strong solution of the initial boundary-value problem which characterizes the Beltrami color flow. We refer to the term strong solutions when we talk about solutions which are functions with some smoothness criteria that we detail below. Let us first introduce few notations: We denote the image domain by Ω. It is a bounded open domain in $\mathbb{R}^2$. We denote by $\partial\Omega$ the boundary of Ω. We define the space-time cylinder $Q_T = \Omega \times (0, T)$, and denote its lateral surface by $S_T = \{(x, t)|x \in$

$\partial\Omega, t \in (0,T)\}$. We define also the parabolic boundary by the union of the bottom and the lateral boundaries of the cylinder $\Gamma_T = \Omega \bigcup S_T$.

The PDE is the gradient descent equation for the Polyakov action as was described in the previous section. We carry out explicitly the result of applying the derivation operator Div. The result is a sum of two terms: The first term results from applying the derivative on $\sqrt{g}G^{-1}$, and the second comes from applying the div on the gradient $div(\nabla U^a) = \Delta U^a$ which is the Laplacian. Remember that the metric, and consequently its inverse and its determinant, depends on first order derivatives. The application of the Div operator on it give rise to second order derivatives of the different channels as well. Rearranging the right hand side of Eq. (3) according to the second order derivatives and the coefficients thereof we arrive to the following coupled system of PDEs:

$$U^a_t = (F^a_{\ b})^{ij} U^b_{x_i x_j}, \quad (x,t) \in Q_T \ , \tag{4}$$

where $a, b = 1,2,3$ are indices in color space, $i, j = 1,2$ are spatial indices and summation is applied on all repeated indices. Note that $(F^a_{\ b})$ are nine 2x2 matrices. Denote by $H^a = U^a_{x_i x_j}$ the Hessian of U^a. This system of PDEs can be written in terms of a trace in spatial domain as

$$U^a_t = \mathrm{Trace}\left(F^a_{\ b} H^b\right) \ , \quad (x,t) \in Q_T \ , \tag{5}$$

where, as before, the repeated b index implies a summation over the color indices. The initial and boundary conditions are

$$U^a(x,0) = U^a_0(x), \quad x \in \Omega \tag{6}$$

$$(F^a_{\ b})\overrightarrow{\nabla} U^b \cdot \overrightarrow{n}\Big|_{S_T} = 0 \quad \text{(no summation on } b \text{ here)}, \tag{7}$$

where $\overrightarrow{n}$ is the outer normal to $\partial\Omega$ and the dot product denotes, as usual, the Euclidian scalar product on $\mathbb{R}^2$.

Lemma 1. *The nine 2x2 matrices $(F^a_{\ b})$ are symmetric, positive definite, and their elements $(F^a_{\ b})^{ij}$ are rational functions of the first derivatives of the different channels. These matrix elements are, moreover, uniformly bounded functions on Q_T.*

Proof. The proof is by direct calculation. One finds for example:

$$\begin{aligned}
\left(F^2_{\ 1}\right)^{11} &= -R_x G_x \frac{g_{22}^2}{g^2} + (R_x G_y + R_y G_x)\frac{g_{12} g_{22}}{g^2} - \frac{R_y G_y}{g}\left(1 + \frac{g_{12}^2}{g}\right) \\
\left(F^2_{\ 1}\right)^{12} &= \left(F^2_{\ 1}\right)^{21} = \frac{R_x G_y + R_y G_x}{g} - \frac{R_x G_y + R_y G_x}{g^2} g_{11} g_{22} - \\
&\qquad \frac{R_x G_y + R_y G_x}{g^2} g_{12}^2 + 2\frac{R_x G_x g_{22} + R_y G_y g_{11}}{g^2} g_{12}^2 \\
\left(F^2_{\ 3}\right)^{22} &= -R_y G_y \frac{g_{11}^2}{g^2} + (R_x G_y + R_y G_x)\frac{g_{11} g_{12}}{g^2} - \frac{R_x G_x}{g}(1 + \frac{g_{12}^2}{g}) \ .
\end{aligned} \tag{8}$$

(here R, G, B denote the three components of the color vector $\overrightarrow{U}$)

These are rational functions of the first derivatives. The diagonal elements are strictly positive (by direct check) and the negativity of the discriminant implies the positive definiteness of this matrix. One can verify by direct check that the coefficients are bounded functions of the first derivatives values. Other matrices are checked along the same lines. □

Next we state the maximum principle for strong solutions of the coupled system of PDEs Eq. (4).

Theorem 1. *Let $\overrightarrow{U_0} \in C^2(\Omega)$ with bounded second derivatives. A solution $\overrightarrow{U} \in C^{2,1}(\bar{Q}_T)$ satisfies, then, the following maximum principle:*

$$\begin{aligned} &1) \quad \max_{\bar{Q}_T} U^a = \max_{\Omega} U_0^a \\ &2) \quad \max_{\bar{Q}_T} \sum_{a=1}^{3} U^a = \max_{\Omega} \sum_{a=1}^{3} U_0^a. \end{aligned} \tag{9}$$

Proof. The proof make use of Lemma 1. We describe here the main steps of the proof. The details can be found in [3]. Note that assertion 1) does not imply, in principle assertion 2). The proof is based on the observation that the off diagonal matrices F^a_b with $a \neq b$ can be written as $U^a_{x_i}$ times a bounded function. It follows that if the maximum is attained in the interior of the cylinder then the first derivatives vanish at that point while the Hessian is negative definite. It implies the negativity of the right side of Eq. (4) while the left side is zero by the maximality of the function at that point. This excludes the interior points. The lateral boundary is shown to be excluded as well by using the Neumann boundary conditions. The upper boundary of the cylinder Q_T is a little more complicated and we leave the details to our technical report [3]. □

This theorem, besides its own value, serves as a basic approximation tool in the proof of the extremum principle for weak solutions of the non-linear system of the color Beltrami flow. We assume in the meantime that weak solutions from a proper space (which will be described below) exist and prove that if they exist, they obey the extremum principle.

4 Extremum Principle for Distributional Solutions

There are two reasons that convinced us to look at weak solutions for the, fairly complicated and highly non-linear, system of the color Beltrami partial differential equations. The first reason is the fact that this is a denoising algorithm. It means that the original image is corrupted with noise. One usually assumes an additive Gaussian or uniform noise. Since the noise is non differential function in ALL its points then one is not allowed to assume that the original noisy image is continuous, let alone differentiable. We consider, therefore, the initial corrupted image to belong to L^∞, i.e. for each color component $U_0^a \in L^\infty(Q_T)$. In order to define a PDE based denoising process, let alone solving it, we have to

work with weak solutions. The second reason is that from the duality viewpoint of Florack [6] images should be considered as linear functionals on the sensor functional space. This space of linear functionals is the dual space, composed of distributions in the sense of Laurent Schwartz [10].

Let us introduce the following notations: We use the following scalar product on Q_T:

$$(u,v) = \int_{Q_T} (uv + u_{x_k} v_{x_k} + u_{x_k x_j} v_{x_k x_j}) dx\, dt$$

This scalar products defines naturally a norm which we denote by $||u|| = \sqrt{(u,u)}$. The Sobolev space of functions, with finite norm, over the cylinder Q_T is defined by $W_2^{2,0}(Q_T) = \{u : Q_T \to \mathbb{R} \big| \ ||u|| < \infty\}$. We will omit from now on the Q_T notation. We write, for example, the above functional space as $W_2^{2,0}$ and remember that all the functions in it are defined over the Q_T cylinder. More generally, the Sobolev space $W_r^{p,q}$ is the space of functions, for which the L_r norm of their first generalized p spatial derivatives and q time derivatives, is finite.

We are now in a position to define weak (generalized) solutions:

Definition 1. *A generalized (weak) solution of the system Eq. (4), with boundary and initial conditions Eqs. (7) and (6), is a vector function $\overrightarrow{U}$ whose components $U^a \in W_2^{2,0}(Q_T)$ for $a = 1,2,3$ and such that for any vector function $\overrightarrow{\eta}$ whose components $(\eta^a) \in W_2^{2,1}(Q_T)$, the following integral equations hold for almost all $t \in [0,T]$:*

$$\int_\Omega U^a \eta^a |_{t=0}^{t=T} \, dx - \int_\Omega U^a \eta_t^a \, dx\, dt = - \int_{Q_T} \left(\eta^a F_b^{a\,ij}\right)_{x_i} U_{x_j}^b. \tag{10}$$

For such weak solutions the following maximum principle holds:

Theorem 2. *Assume $\overrightarrow{U}_0 \in L^\infty(Q_T)$. For a weak (distributional) solution $\overrightarrow{U} \in W_2^{2,0}(Q_T)$ of the system (4),(6),(7) we have for almost all $(x,t) \in Q_T$:*

$$ess \inf_\Omega |U_0^a(x)| \le |U^a(x,t)| \le ess \sup_\Omega |U_0^a(x)|, \tag{11}$$

$$ess \inf_\Omega |\sum_{a=1}^3 U_0^a(x)| \le |\sum_{a=1}^3 U^a(x,t)| \le ess \sup_\Omega |\sum_{a=1}^3 U_0^a(x)|. \tag{12}$$

Remark that by definition :
$ess \sup_{x \in X} f(x) = \inf_{A_0 \subset S_0} (\sup_{X - S_0} f(x)), \quad where \quad S_0 = \{S \subset X | \mu(S) = 0\}$

Proof. The proof is based on Sobolev Embedding Theorem [4] (by which the space $W_2^{2,0}(Q_T)$ is embedded in $C(\bar{Q}_T)$) and on a Density Theorem [5] (which asserts that the space $W_2^{2,0}(Q_T) \bigcap C^\infty(\bar{Q}_T)$ is dense in the space $W_2^{2,0}(Q_T)$).

By the density theorem we can approximate the solution $\overrightarrow{U}$ by smooth vector functions $\overrightarrow{U_k} \in W_2^{2,0}(Q_T) \bigcap C^\infty(\bar{Q}_T)$ such that $||U_k^a - U^a||_{W_2^{2,0}(Q_T)} \to 0$ as

$k \to \infty$. The initial data $\overrightarrow{U_0}$ can also be approximated by smooth functions $\overrightarrow{\Phi_k} \in C^\infty(\Omega)$, such that $\Phi_k^a \to U_0^a$ uniformly as $k \to \infty$. Now for each k consider the boundary value problem (4),(6),(7) corresponding to the vector function $\overrightarrow{U_k}$. For enough smooth solution of this problem, based on Theorem 9 we have the maximum principle: $|U_k^a| \leq \sup\limits_{\Omega} |\Phi_k^a|$. Furthermore, by the Embedding Theorem there exists a constant C such that

$$|U^a| \leq ess\sup_{Q_T} |U_k^a - U^a| + ess\sup_{Q_T} |U_k^a| \leq C \cdot ess\sup_{Q_T} ||U^a - U_k^a||_{W_2^{2,0}(Q_T)} + ess\sup_{\Omega} |\Phi_k^a|$$

$$\leq C \cdot ess\sup_{Q_T} ||U^a - U_k^a||_{W_2^{2,0}(Q_T)} + ess\sup_{\Omega} |U_0^a| + ess\sup_{\Omega} |U_0^a - \Phi_k^a|.$$

Letting $k \to \infty$, we obtain the maximum principle for the weak solutions from $W_2^{2,0}$:

$$|U^a| \leq ess\sup_{\Omega} |U_0^a|. \tag{13}$$

In a similar way one obtains (12). □

5 The Discrete Maximum Principle and Stability

In this section we show that the commonly used central difference second order explicit schemes violate, in general, the discrete maximum principle. We give nevertheless, for these schemes, a theoretical proof of stability.

We work on a rectangular grid

$$x_i = i\Delta x, \quad y_j = j\Delta y, \quad t_m = m\Delta t,$$

$$i, j = 0, 1, 2, ...M; \quad m = 0, 1, 2, ...[T/\Delta t]$$

The spatial units are normalized such that $\Delta x = \Delta y = 1$. The approximate solution $(R_{ij}^m, G_{ij}^m, B_{ij}^m)$ samples the functions:

$$R_{ij}^m \equiv U^1(i\Delta x, j\Delta y, m\Delta t),$$

$$G_{ij}^m \equiv U^2(i\Delta x, j\Delta y, m\Delta t),$$

$$B_{ij}^m \equiv U^3(i\Delta x, j\Delta y, m\Delta t),$$

On the boundary we impose the Neumann boundary condition. This corresponds to a prolongation by reflection of the image across the boundary.

We replace the second spatial derivatives and the first time derivative by central difference and forward difference respectively. Based on (3), the first equation of the system (4),(6),(7) can be written in the form

$$U_t^1 = \frac{1}{\sqrt{g}} \mathrm{Div}(D\nabla U^1) \ . \tag{14}$$

The diffusion matrix is written here as

$$D = \begin{pmatrix} a & b \\ b & c \end{pmatrix}$$

where the coefficients are given in terms of the image metric: $a = g_{22}/\sqrt{g}$; $c = g_{11}/\sqrt{g}$; $b = -g_{12}/\sqrt{g}$. With this notation,thus, equation (14) is written as

$$U_t^1 = \frac{1}{\sqrt{g}}((aU_x^1 + bU_y^1)_x + (bU_x^1 + cU_y^1)_y) \ . \tag{15}$$

We approximate Eq. (15) by the following central difference explicit scheme :

$$R_{ij}^{m+1} = R_{ij}^m + \beta \Delta t O_{ij}(R^m, G^m, B^m) \tag{16}$$

where $O_{ij}(R^m, G^m, B^m)$ is the discrete version of the right side of Eq. (4) and is given explicitly, in the central difference framework, by

$$\begin{aligned} O_{ij} \ = \ & \\ & \frac{1}{\sqrt{g}}\Big[a^m_{i+\frac{1}{2},j}(R^m_{i+1,j} - R^m_{i,j}) - a^m_{i-\frac{1}{2},j}(R^m_{i,j} - R^m_{i-1,j}) \\ & + c^m_{i,j+\frac{1}{2}}(R^m_{i,j+1} - R^m_{i,j}) - c^m_{i,j-\frac{1}{2}}(R^m_{i,j} - R^m_{i,j-1}) \\ & + \frac{1}{4}b^m_{i,j+1}(R^m_{i+1,j+1} - R^m_{i-1,j+1}) - \frac{1}{4}b^m_{i,j-1}(R^m_{i+1,j-1} - R^m_{i-1,j-1}) \\ & + \frac{1}{4}b^m_{i+1,j}(R^m_{i+1,j+1} - R^m_{i+1,j-1}) - \frac{1}{4}b^m_{i-1,j}(R^m_{i-1,j+1} - R^m_{i-1,j-1})\Big] \ , \end{aligned} \tag{17}$$

where the half indices are obtained by linear interpolation. The equations for the two other color components are discretized in the same manner. This scheme is stable under CFL-like bound requirements of the step time. The stability, as well as the lack of extremum principle property, can be learned from the following theorem.

Theorem 3. *If Δt satisfies the condition :*

$$\Delta t \leq \frac{1}{8\beta \max_{i,j}\{\frac{a_{i+\frac{1}{2},j}}{\sqrt{g_{i,j}}}, \frac{a_{i-\frac{1}{2},j}}{\sqrt{g_{i,j}}}, \frac{c_{i,j+\frac{1}{2}}}{\sqrt{g_{i,j}}}, \frac{c_{i,j-\frac{1}{2}}}{\sqrt{g_{i,j}}}\}}, \tag{18}$$

then the solution satisfies :

$$\begin{aligned} |R^m_{i,j}| &\leq e^{\alpha t_m} \max_{i,j} |R^0_{i,j}|, \\ |G^m_{i,j}| &\leq e^{\alpha t_m} \max_{i,j} |G^0_{i,j}|, \\ |B^m_{i,j}| &\leq e^{\alpha t_m} \max_{i,j} |B^0_{i,j}|, \end{aligned}$$

$$\textit{where} \quad \alpha = 2\beta \max_{ij} \frac{|b^m_{ij}|}{\sqrt{g^m_{ij}}} \leq 2\beta.$$

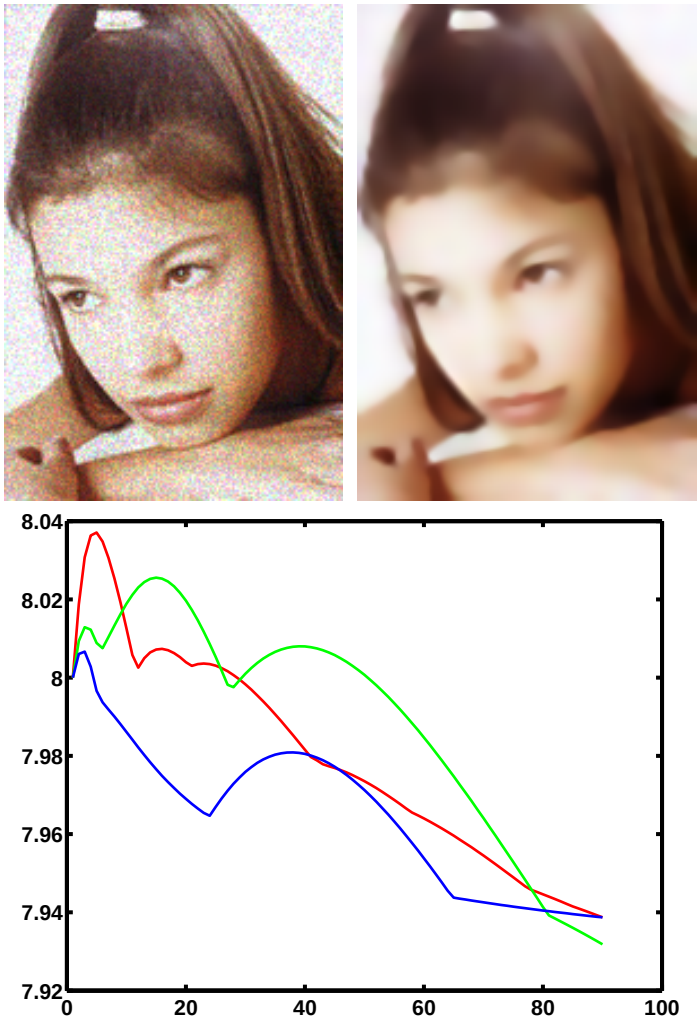

Fig. 1. Top-left: Noisy Camila image. Top-right: Result of the Beltrami flow after 90 iteration. Bottom: Plot of maximum of each of the channels versus number of iterations.Parameters: $\beta^2 = 100$, first scheme: $\Delta t = 0.0091$.

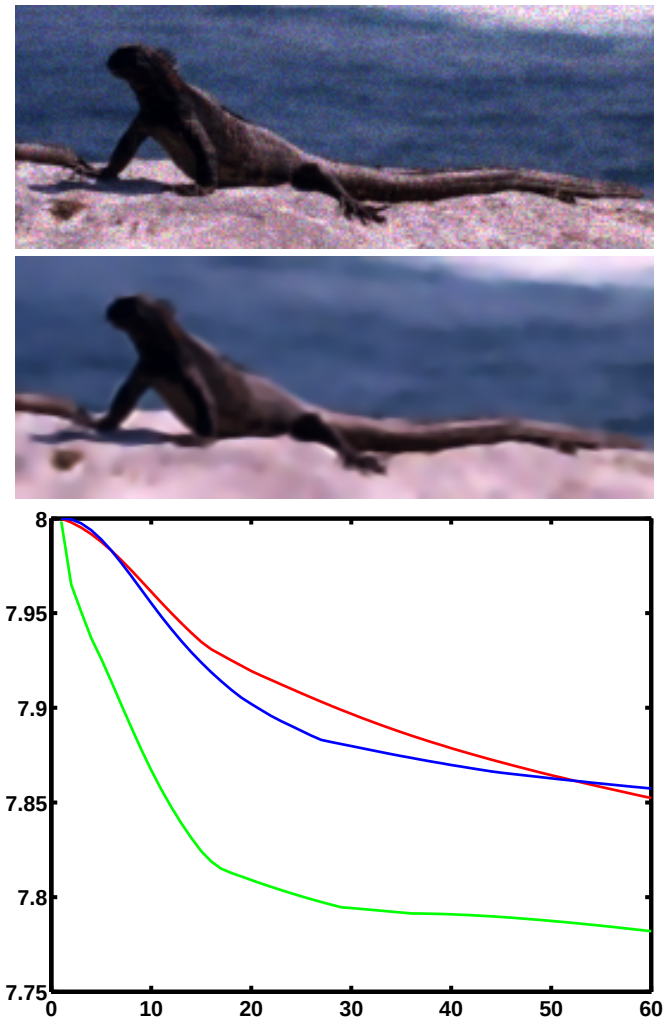

Fig. 2. Top: Noisy Iguana image. Middle: Denoised Iguana by the Beltrami flow with after 60 iterations. Bottom: Plot of maximum of each of the channels versus number of iterations. Parameters: β^2=80, $\Delta t = 0.0091$.

Proof. See details in [3] □.

The inequalities in Theorem 3 show that the numerical solution is bounded in each iteration by the maximum value of the initial image multiplied by a factor. It guarantees that the flow does not blow up in finite time and ensures its stability. At the same time it is clear from the positivity of β that the maximum principle can possibly be violated. One can actually see it in practice (see Fig. 1).

The reason for this discrepancy between the continuous and discrete setting is the fact that this second order approximation is not a non-negative one. Indeed, the mixed derivatives in eq. (15) can create negative weights in certain pixels. One can easily show that a scheme which is based on a nonnegative discretization does satisfy the discrete maximum principle. Based on this result, the problem of proving the discrete maximum principle boils down to the problem of finding a nonnegative second order difference approximation. In [18], Weickert proposed a way for building a nonnegative scheme. The non-negativity of his proposed scheme depends, though, on the condition number of the diffusion tensor D. Only in pixels were the condition number is smaller than $3 + 2\sqrt{2}$ the weights are non-negative. This limits the application of the scheme since in many images the condition number is typically higher than this limit in many pixels.

6 Details of the Implementation and Results

We present in this Section results that represent the numerical behavior of the above described numerical scheme. The initial data is given in three channels r, g and b in the range 0 to 256. We first transfer the images to the more perceptually adaptive coordinates $R = \log(1+r)$, $G = \log(1+g)$, $B = \log(1+b)$. The dynamic range for these variables is 0 to 8 and these adaptive coordinates do not limit the generality of our analysis. In the two examples presented below we corrupt an image with random noise and denoise it using the scheme mentioned above.

In the implementation, the parameters β and Δt were chosen to satisfy the stability condition Eq. (18).

Figure 2 demonstrates that the violation of the maximum principle does not obligatory occur in the central difference scheme. In this figure the numerical scheme respects the maximum principle.

Remark that for a too large time step one gets a violation of the maximum principle in the Iguana image as well. Yet this violation gets smaller and smaller until the maximum principle is satisfied as the time step becomes smaller and smaller. This is NOT the case for the Camila image where the break up of the maximal principle is stable and does not depend on the time step. It is not clear for us what are the special characteristic of an image that make it to respect or not the discrete maximum principle.

7 Concluding remarks

We have studied in this paper the extremum principle condition for the color image Beltrami flow. This is done in the context of the possibility to build a scale-

space from the solution to this complicated non-linear coupled system of PDEs. We adapted in this paper the duality paradigm of Florack and we regarded "true images" as tempered distributions. We investigate therefore, besides the strong solutions, the generalized (weak) solutions. We proved that both the strong and the weak solutions satisfy the extremum principle which is a necessary condition for causality, and therefore, for the construction of well-defined scale-space.

We addressed also the problem of numerically construct a well-defined scale-space. It is shown that, in contrast to the continuous case, the extremum principle is not automatically guaranteed. We prove that the central difference scheme *does not* guaranty the satisfaction of the extremum principle. It is important to note that we studied many variants of central and/or forward-backward schemes. They all shared similar behavior and the detailed description of these and other methods will be found in future work.

Acknowledgments

This research has been supported in part by the Israel Academy of Science, Tel-Aviv University fund, the Adams Center and the Israeli Ministry of Science.

References

1. L. Alvarez, P.L. Lions, J.M. Morel,"Image selective Smoothing and edge detection by Nonlinear Difusion.II", *Siam Journal on Numerical Analysis*, Vol.29, Issue (1992), 845-866.
2. F. Catte, P. L. Lions, J. M. Morel and T. Coll, "Image selective smoothing and edge detection by nonlinear diffusion", SIAM J. Num. Anal., vol. 29, no. 1, pp. 182-193, 1992.
3. L. Dascal and N. Sochen, "The Maximum principle for Beltrami color flow", Technical Report Tel-Aviv University, Israel, in preparation.
4. D.Gilbarg, N.Trudinger, "Elliptic partial differential equations of second order",Springer-Verlag, 1977.
5. L.Evans, "Partial differential equations",Berkeley Mathematics 1994.
6. L. Florack, "Duality principles in Image processing and Analysis", IVCNZ 1998.
7. R. Kimmel and R. Malladi and N. Sochen, "Images as Embedding Maps and Minimal Surfaces: Movies, Color, Texture, and Volumetric Medical Images", International Journal of Computer Vision 39(2) (2000) 111-129.
8. R. Kimmel and N. Sochen, "Orientation Diffusion or How to comb a Porcupine", *Journal of Visual Communication and Image Representation* 13:238-248, 2001.
9. L. Rudin, S. Osher and E. Fatemi, " Non Linear Total Variation Based Noise Removal Algorithms", *Physica D 60 (1992) 259-268.*
10. L. Schwartz, "Functional analysis", Courant Institute of Mathematical Sciences, 1964.
11. J.J. Koenderink, "The structure of image", Biol. Cybern., Vol.50, 36-370, 1984.
12. A. M. Polyakov, "Quantum geometry of bosonic strings", *Physics Letters*, **103B** (1981) 207-210.
13. N. Sochen and R. Kimmel and R. Malladi, "From high energy physics to low level vision", Report, LBNL, UC Berkeley, LBNL 39243, August, Presented in ONR workshop, UCLA, Sept. 5 1996.

14. N. Sochen and R. Kimmel and R. Malladi, "A general framework for low level vision", *IEEE Trans. on Image Processing*, 7 (1998) 310-318.
15. N. Sochen and Y. Y. Zeevi, "Representation of colored images by manifolds embedded in higher dimensional non-Euclidean space", Proc. IEEE ICIP'98, Chicago, 1998.
16. N. Sochen and Y. Y. Zeevi, "Representation of images by surfaces embedded in higher dimensional non-Euclidean space", 4th International Conference on Mathematical Methods for Curves and Surfaces, Lillehamer, Norway, July 1997.
17. R. Kimmel and N. Sochen. "Orientation Diffusion or How to Comb a Porcupine ? ", Special issue on PDEs in Image Processing, Computer Vision, and Computer Graphics, Journal of Visual Communication and Image Representation. In press.
18. J. Weickert, " Anisotropic Diffusion in Image processing", Teubner Stuttgart, 1998.
19. J.Weickert,"Coherence-enhancing diffusion of color images", Image and Vision Computing, Vol.17, 201-212, 1999.
20. S. Di Zenzo ," A note on the gradient of a multiimage", Computer Vision, Graphics and Image Processing, 33:116-125, 1986.